

# Optimization of a PDMS structure for energy harvesting under compressive forces

Shi, J. , Zhu, D. , Cao, Z. and Beeby, S. P.

Published PDF deposited in [Curve](#) March 2016

**Original citation:**

Shi, J. , Zhu, D. , Cao, Z. and Beeby, S. P. (2015) Optimization of a PDMS structure for energy harvesting under compressive forces. Journal of Physics: Conference Series, volume 660 (1): 012041

URL: <http://dx.doi.org/10.1088/1742-6596/660/1/012041>

DOI: 10.1088/1742-6596/660/1/012041

Publisher: IOP Publishing

**Content from this work may be used under the terms of the Creative Commons Attribution 3.0 licence. Any further distribution of this work must maintain attribution to the author(s) and the title of the work, journal citation and DOI.**

**Copyright © and Moral Rights are retained by the author(s) and/ or other copyright owners. A copy can be downloaded for personal non-commercial research or study, without prior permission or charge. This item cannot be reproduced or quoted extensively from without first obtaining permission in writing from the copyright holder(s). The content must not be changed in any way or sold commercially in any format or medium without the formal permission of the copyright holders.**

**CURVE is the Institutional Repository for Coventry University**

## Optimization of a PDMS structure for energy harvesting under compressive forces

This content has been downloaded from IOPscience. Please scroll down to see the full text.

2015 J. Phys.: Conf. Ser. 660 012041

(<http://iopscience.iop.org/1742-6596/660/1/012041>)

View [the table of contents for this issue](#), or go to the [journal homepage](#) for more

Download details:

IP Address: 194.66.32.16

This content was downloaded on 29/03/2016 at 16:20

Please note that [terms and conditions apply](#).

# Optimization of a PDMS structure for energy harvesting under compressive forces

J Shi<sup>1</sup>, D Zhu<sup>2</sup>, Z Cao<sup>1</sup> and S P Beeby<sup>1</sup>

<sup>1</sup> Electronics and Electrical Engineering Group, Electronics and Computer Science University of Southampton, Southampton, SO17 1BJ, UK

<sup>2</sup> School of Computing, Electronics and Maths, Faculty of Engineering, Environment and Computing, Coventry University, Coventry, CV1 5FB

E-mail:js4g11@soton.ac.uk

**Abstract.** This paper reports the optimisation of a PDMS structure for energy harvesting applications. The PDMS structure was optimised using ANSYS simulation. The fabrication processes were also optimised for maximum PDMS ferroelectret energy harvesting performance. The optimised PDMS structure was fabricated using a 3D-printed plastic mould. The ANSYS simulation and experiment results demonstrated the variation in energy harvesting performance of the PDMS ferroelectret depending upon the different void geometry. The optimised operating frequency is determined by the geometry of the voids inside ferroelectrets and the Young's modulus of the PDMS. The peak voltage and energy generated per strike under a compressive load was obtained experimentally as a function of force applied and frequency. The experimental maximum peak output power of an optimised PDMS structure with an area of  $2 \times 2 \text{ cm}^2$  was  $0.46 \mu\text{W}$  across an optimum load resistance of  $21 \text{ M}\Omega$  under a square wave force of  $800 \text{ N}$  and  $17 \text{ Hz}$ .

## 1. Introduction

Ferroelectrets are thin films of polymer foams which can store electric charges in its internal voids, presenting strong piezoelectric-like properties after electric charging [1]. They are able to generate an electric signal during compressive and bending deformations. Due to its high piezoelectric properties, ferroelectrets have already been utilized extensively in sensor or transducer applications, such as microphones, headphones and loudspeakers [2-4].

With the development in the field of wearable electronics, there is a demand for energy supplies, more specifically renewable, long life time energy sources. Kinetic energy harvesting technology that gathers energy from human motion, such as running and walking or ambient vibration, such as machinery vibration, has received growing attention over the last decade. This technology enables wearable devices to be operated using the power that is harvested from human activities. A common approach to harvest energy from human motion is utilizing piezoelectric effect that converts mechanical energy to electrical energy. Commonly, investigated piezoelectric materials for kinetic energy harvesting are lead zirconate titanate (PZT) and polyvinylidene fluoride (PVDF). Even though PZT has relatively high piezoelectric charge constant  $d_{33}$ , its high Young's modulus ( $63 \text{ GPa}$ ) is unsuitable for wearable applications. On the other hand, PVDF has low Young's modulus ( $2.9 \text{ GPa}$ ), which makes suitable for wearable energy harvesting. But, its  $d_{33}$  is an order of magnitude lower than that of PZT. Comparing with these two piezoelectric materials, ferroelectrets are light, thin, soft material and have a



relatively high  $d_{33}$  that is comparable to PZT. These properties make it possible for using ferroelectrets as the active material to harvest energy from human motion and power wearable electronic devices.

The piezoelectric like properties of ferroelectrets has already been theoretically analysed [5, 6]. However, most ferroelectrets are formed by a modified film blow and extrusion process for producing the desired cellular structures. The results of this fabrication method are usually ill-controlled in both individual void geometry and overall cellular structure. Furthermore, the existing modelling methods to approximate the piezoelectric like properties of these materials and structures are simplified models that do not consider individual void geometry and void distribution. We have develop a model that predicts the variation in performance of PDMS ferroelectret with different void geometries [7]. This paper presents the optimization, fabrication and testing of an optimized PDMS ferroelectret material for energy harvesting applications.

### 2. Operating principle

As illustrated in Figure 1, the structure consists of top and bottom electrodes, and two void layers inside. When a force is applied to a charge-implanted cellular film, the thickness of the film, as well as the induced charge density on the top and bottom electrodes will change, which results in the piezoelectric-like effect. An analytical model has been developed to investigate the material properties of the composite structures, with key parameters estimated by ANSYS simulation. Equation (1) and (2) show the relationships between its piezoelectricity and the composite structures.

$$d_{33} = n(n + 1)\epsilon_1\sigma tr_1(1 - sr_1)^2[sr_1[(n + 1) + n\epsilon_1 tr_1]^2 c_{33}]^{-1} \tag{1}$$

$$d_{31} = n(n + 1)\epsilon_1\sigma tr_1(1 - sr_1)(sr_2 - 1)\gamma[n(n + 1)\epsilon_1\sigma tr_1(1 - sr_1)(sr_2 - 1)\gamma]^{-1} \tag{2}$$

Where  $\epsilon_1$  is the relative dielectric constant of PDMS;  $n$  is the number of void layers;  $c_{33}$  is the elastic modulus of PDMS;  $\sigma$  is the charge density on void surface;  $\gamma$  is the Poisson’s ratio;  $x_1$  and  $x_2$  are the thickness of solid and void layers, respectively;  $sr_1$  and  $sr_2$  are dimensions  $A_2$  divided by  $A_1$  and  $A_4$  divided by  $A_3$ , respectively;  $tr_1$  is dimension  $x_2$  divided by  $x_1$ .

According to Paschen’s law [8], the breakdown voltage for void is described by the equation

$$V_b = apx_2[\ln(pd) + b]^{-1} \tag{3}$$

Where  $V$  is the breakdwon voltage;  $p$  is the gas pressure in the void;  $x_2$  is the void height;  $a$  and  $b$  are constants which depend upon the composition of the gas.

Results from the model are presented in Figure 4 and Figure 6.

### 3. Fabrication processes and experiment

#### 3.1. Fabrication process for PDMS ferroelectret

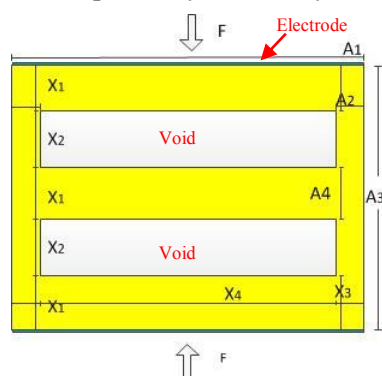


**Figure 1.** A model for the piezoelectricity of a charge-implanted composite microstructure

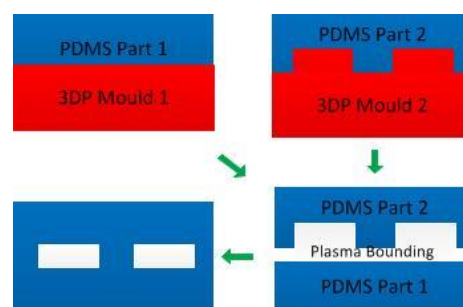


**Figure 2.** Schematic of fabrication processes

The PDMS ferroelectrets used in the test is fabricated using a moulding process as illustrated in Figure 2. The plastic moulds were 3D- printed by a Connex350 TM 3D printing system (Stratasys, MN, USA). The VerClear™ was selected as the mould material because it is transparent, which makes it easy to observe the entire fabrication process. Because the 3D printable material inhibits PDMS polymerization

and the printed structure tends to warp to some extent when it is removed from the printer, the resulting 3D-printed mould is not immediately suitable for PDMS casting. The moulds must be baked in an oven at 80 °C for 24 hours. Next, the moulds were placed and glued using a drop of degassed non-polymerized PDMS to a piece of clear glass, with its base in contact with the PDMS film. After this step, the glass-backed moulds were exposed to a silane vapour for 1 hour to be coated with a thin layer of trichloro(1H,1H,2H,2H-perfluorooctyl)silane (Sigma Aldrich, MO, USA) with promote of the PDMS.

Once the plastic moulds are fabricated, liquid PDMS and curing agent (Sylgard 184 from Dow Corning, MI, USA) were mixed at a 10:1 weight ratio and this mixture was degassed in a vacuum desiccator. The degassed PDMS was poured into the glass-backed mould which were again degassed and then baked at 80 °C for 1 hour. When the degassed PDMS was poured into the mould, the fluid level in the mould was monitored to ensure the degassed PDMS would not overflow. This step is used to control the thickness of the PDMS. After detaching the polymerized PDMS from the moulds, an oxygen plasma treatment was applied on the patterned surface of one PDMS layer and the smooth surface of the other PDMS layer (Femto Asher, Diener, Germany, 30 S at 35-40W) and these were then bonded together. The bonded PDMS was then baked in oven at 80 °C for 1 hour. A 10 N force was applied to the sample during the bake to improve the bonding effect, and also recover the original hydrophobic PDMS surface chemistry. The image of a fabricated PDMS ferroelectret is shown in Figure 3. After the fabrication, the sample was charged using a corona charging method. For this experiment, corona charging was applied at room temperature and normal atmospheric pressure. A corona-tip voltage of -25 kV and a charging time of 2 mins were employed.

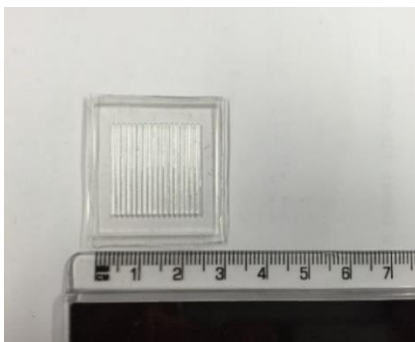


**Figure 3.** Image of ferroelectret material

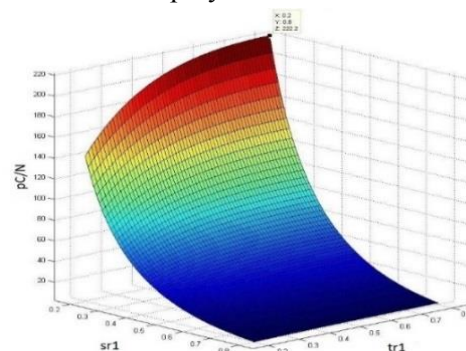


**Figure 4.** Analytical rectangle model results varying with the size of voids [7]

### 3.2. Testing

To investigate how the properties of the material are affected by the void structure, three different structures were designed, basing upon the maximum precision of the 3D printer, the restrictions of fabrication process and analytical results (Figure 4). From the Figure 4, the analytically modelled piezoelectric properties of the PDMS ferroelectret are improved with an increase of the void area and the optimized structure was achieved with a ratio  $tr_1=0.8$  for a single void layer of PDMS ferroelectret material [7]. The detailed structural parameters are shown in table 1. To quantify the applied forces on the test samples, an Instron electrodynamic instrument (ElectroPuls E1000, Instron Ltd) was used. The maximum dynamic force this equipment can produce is 1000 N and it can provide several types of compressive force including square, sinusoidal and triangular wave forces. The frequency of the compressive forces applied on the test samples was varied from 0 to 100 Hz. These parameters can be modified in the control software.

The output voltages of the PDMS ferroelectret under square wave compressive force were recorded using an oscilloscope. In order to calculate the output energy from the voltage signal, the measurement outputs were transferred from the oscilloscope to a computer and analysed. In addition, the material was also characterized by measuring the output voltage pulses, whilst scanning the load resistance from 1M $\Omega$  to 51M $\Omega$ .

**Table 1.** The dimensions for three designed void structures

|             | $Tr_1$ | $Sr_1$ | Thickness<br>(Solid layer) | Thickness<br>(Void layer) | Width<br>(Void) | Width<br>(Void gap) | Natural frequency<br>(ANSYS) |
|-------------|--------|--------|----------------------------|---------------------------|-----------------|---------------------|------------------------------|
| Structure 1 | 0.8    | 0.4    | 0.4mm                      | 0.32mm                    | 0.75mm          | 0.5mm               | 24Hz                         |
| Structure 2 | 0.8    | 0.4    | 2mm                        | 1.6mm                     | 0.75mm          | 0.5mm               | 21Hz                         |
| Structure 3 | 0.8    | 0.5    | 2mm                        | 1.6mm                     | 0.625mm         | 0.625mm             | 22Hz                         |

#### 4. Results and Discussion

The output voltage of the ferroelectret PDMS film under compressive force takes the form of a voltage pulse as shown in Figure 5. From this figure, the maximal peak voltage was measured after 1 hour and 100 hours after poling and were 0.9 V and 0.48 V, respectively. Thus device voltage is reduced by around 47% after 99 hours. This high decay ratio is related to the poor charge stability at the PDMS/air interface.

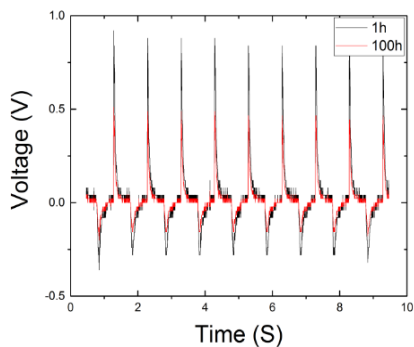


**Figure 5.** Measured voltage output of structure 1 from a 800 N compressive force, 1 Hz frequency, and 21 MΩ load resistance

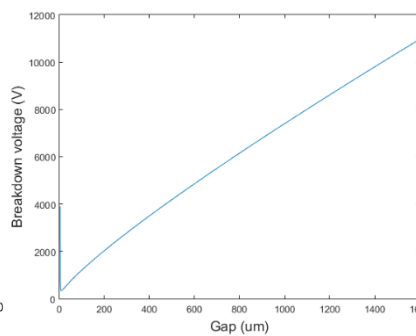


**Figure 6.** Analytical minimum breakdown voltage as function of the void height

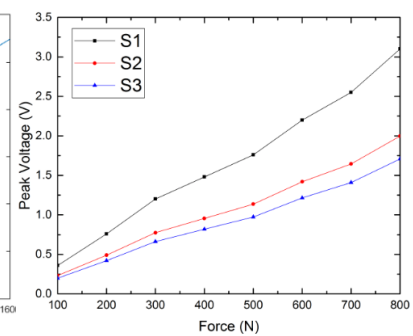


**Figure 7.** Measured voltage output of from 100 to 800 N compressive force at 17 Hz and 21 MΩ load resistance

Figure 6 shows the minimum required breakdown voltage to achieve polarization for different void height. With the void thickness height, ferroelectret requires a higher voltage to polarize. The thinner ferroelectret can achieve a higher surface charge density than thicker ferroelectret based on the same poling voltage resulting in higher piezoelectric-like properties.

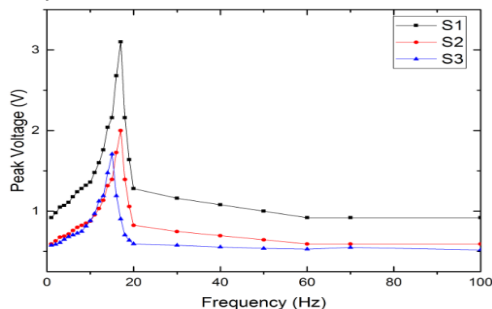
Figure 7 shows the peak output voltage at different applied forces with the frequency of 17 Hz and load resistance of 21 MΩ for these three samples. The output voltage steadily increases with increasing applied force and the maximum peak voltage is achieved at 800 N for these samples.

Figure 8 shows the peak output voltage of the three samples at different frequencies. The output peak voltage initially increases with increasing applied frequency and then start to decline at 17Hz. The optimized operating frequencies are closed to the first natural frequencies which are defined by the geometry and stiffness of materials. The thinner film have higher optimized operating frequency while the lower effective area ratio can reduce the frequency.

Figure 9 shows the characteristic I-P curves of the three PDMS films under 800 N compressive forces with the frequency of 17 Hz, as a function of load resistance. From the figure, it can be observed that the maximum peak power of 0.46 μW can be achieved from the structure 1 PDMS ferroelectret on 21 MΩ load resistance at 17 Hz. These results indicated that the lower effective area ratio and thinner PDMS ferroelectret can produce more output power. Both theoretical and experimental results indicate



that a thinner PDMS ferroelectret will also further enhance the charge long term reliability and charge density.



**Figure 8.** Measured voltage output under 800 N compressive force at different frequency, and 21 MΩ load resistance

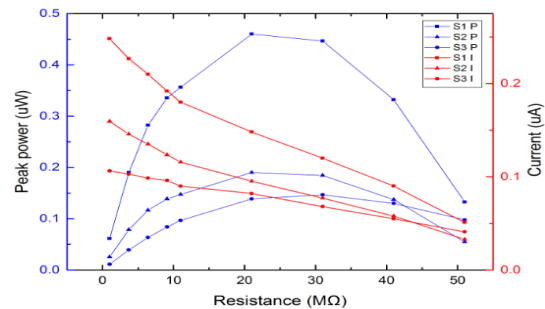


**Figure 9.** Power-resistance trace of PDMS material under 800 N compressive force and 17 Hz force frequency

## 5. Conclusion

In this work, the simulation, fabrication and testing of PDMS ferroelectrets with a variety of dimensions has been investigated. The energy harvesting properties of PDMS ferroelectret are improved with an increase in void area and thinner total thickness as predicted by the model. In addition, the operating frequencies can significantly affect the output power. The optimized operating frequency is achieved at the natural frequency which is determined by the geometry of material. This needs to be taken into consideration when designing the power electronics for the energy harvester. The optimized PDMS ferroelectret with the size of 2 cm x 2 cm generates a maximum of 3.1 V, 0.46 μW when connected to a 21 MΩ resistive load under a square compressive force of 800 N at 17 Hz. This equals a power density of 0.12 μW/cm<sup>2</sup>. Future work will focus on improving the charge density, stability and integrated in wearable devices.

## Acknowledgements

This work was performed under the SPHERE IRC funded by the UK Engineering and Physical Sciences Research Council (EPSRC), Grant EP/K031910/1. Prof Beeby would also like to acknowledge his EPSRC Fellowship, Grant EP/1005323/1

## References

- [1] G. M. Sessler, "Charge distribution and transport in polymers", *IEEE Trans. Dielectr. Electr. Insul.*, Vol. 4, No.5, pp. 614-628, 1997.
- [2] S. Bauer, R. Gerhard-Multhaupt, and G.M. Sessler, "Ferroelectrets: Soft electroactive foams for transducers," *Physics Today* vol. 57, no. 2, pp. 37-43, 2004
- [3] M. Paajanen, "The cellular polypropylene electret material – Electromechanical properties," *D. Tech. Dissertation, VTT Publications*, Vol. 436, Espoo, 2001.
- [4] Michael Wegener and Werner Wirges "Optimized Electromechanical Properties and Applications of Cellular Polypropylene - a New Voided Space-Charge Electret Material" *The Nano-Micro Interface* (H.-J. Fecht, M. Werner, Editors) (WILEY-VCH, Weinheim, 2004) pp. 303-317 (2004).
- [5] J. Hillenbrand and G. M. Sessler, "Piezoelectricity in cellular electret films", *IEEE Trans. Dielect. Electr. Insul.*, vol. 7 (4), pp. 537-542, 2000.
- [6] M. Paajanen, J. Lekkala, and H. Välimäki, "Electromechanical modeling and properties of the electret film EMFi", *IEEE Trans. Dielect. Electr. Insul.*, vol. 8 (4), pp. 629-636, 2001.
- [7] Shi, J, Zhu, D and Beeby, S.P. "An investigation of PDMS structures for optimized ferroelectret performance". *Journal of Physics: Conference Series*, 557, 012104. 2014.
- [8] Lieberman, M. A., & Lichtenberg, A. J. "Principles of plasma discharges and materials processing." *MRS Bulletin*, 30, 899-901. 1994